GE-QUANTUM DOTS ON SI(001) TAILORED BY CARBON PREDEPOSITION

O. LEIFELD [*,**], D. GRÜTZMACHER[*], B. MÜLLER [***], K. KERN [**]
[*] Micro- and Nanostructures Laboratory, Paul-Scherrer-Institute, CH-5232 Villigen-PSI,
[**] Institut de Physique Expérimentale, EPFL, CH-1015 Lausanne, Switzerland
[***] Institute of Quantum Electronics, Nonlinear Optics Laboratory, ETHZ, CH-8093 Zürich, Switzerland

ABSTRACT

The morphology of Si(001) after carbon deposition of 0.05 to 0.11 monolayers (ML) was investigated in situ by ultra-high vacuum scanning tunneling microscopy (UHV-STM). The carbon induces a c(4x4)-reconstruction of the surface. In addition, carbon increases the surface roughness compared to clean Si(001) (2x1). In a second step, the influence of the carbon induced restructuring on Ge-island nucleation was investigated. The 3D-growth sets in at considerably lower Ge coverage compared to the clean Si(001) (2x1) surface. This leads to a high density of small though irregularly shaped dots, consisting of stepped terraces, already at 2.5 ML Ge. Increasing the Ge-coverage beyond the critical thickness for facet formation, the dots show {105}-facets well known from Ge-clusters on bare Si(001) (2x1). However, they are flat on top with a (001)-facet showing the typical buckled Ge rows and missing dimers. This indicates that the compressive strain is not fully relaxed in these hut clusters.

INTRODUCTION

Self organized quantum dots can be manufactured in many heteroepitaxial systems, driven by stress relaxation due to lattice mismatch. In the Si/Ge system, small optically active 3-D dots may be a viable route towards new Si-based optoelectronic devices. Recently small Ge dots (10 nm) showing strong photoluminescence were fabricated at temperatures as high as 550°C by MBE using Si(001) substrates with submonolayer C pre-deposition [1]. Their structural properties, however, were not revealed in detail. The aim of this paper is a detailed examination of the surface morphologies that occur in connection with the growth of these C-induced Ge-quantum dots by in-situ STM. This includes the investigation of the submonolayer C-coverages on Si(001) (2x1) as such, as this is a prerequisite for the understanding of the dot layer growth.

EXPERIMENT

Setup

For the investigations we have realized a combination of an STM with our MBE/UHV-CVD machine. The growth system is composed of a Balzers UMS 500 MBE-chamber combined with a UHV-CVD-reactor, both allowing processing of 4-inch samples. A schematic drawing is shown in Fig.1. Up to 5 wafers are introduced via one of the loadlock chambers and are distributed from there by means of the sample transfer system (sample handler) to the various locations. The MBE-chamber is equipped with electron beam evaporators for Si and Ge and resistively heated evaporation crucibles for Sb and B dopants. Carbon is sublimated from a well-shielded DC-heated pyrolytic graphite filament The substrate temperature of the 4-inch wafer can be varied from room temperature (RT) up to 1000°C. Substrate rotation provides homogeneous film thickness over the wafer surface. The 4-inch wafer STM is contained in a transportable ultra high vacuum (UHV) chamber, which is attached to the sample transfer chamber of the MBE/CVD-system via a small transfer lock between two CF150 gate valves, as seen in Fig.1. Processed wafers are

Mat. Res. Soc. Symp. Proc. Vol. 533 © 1998 Materials Research Society

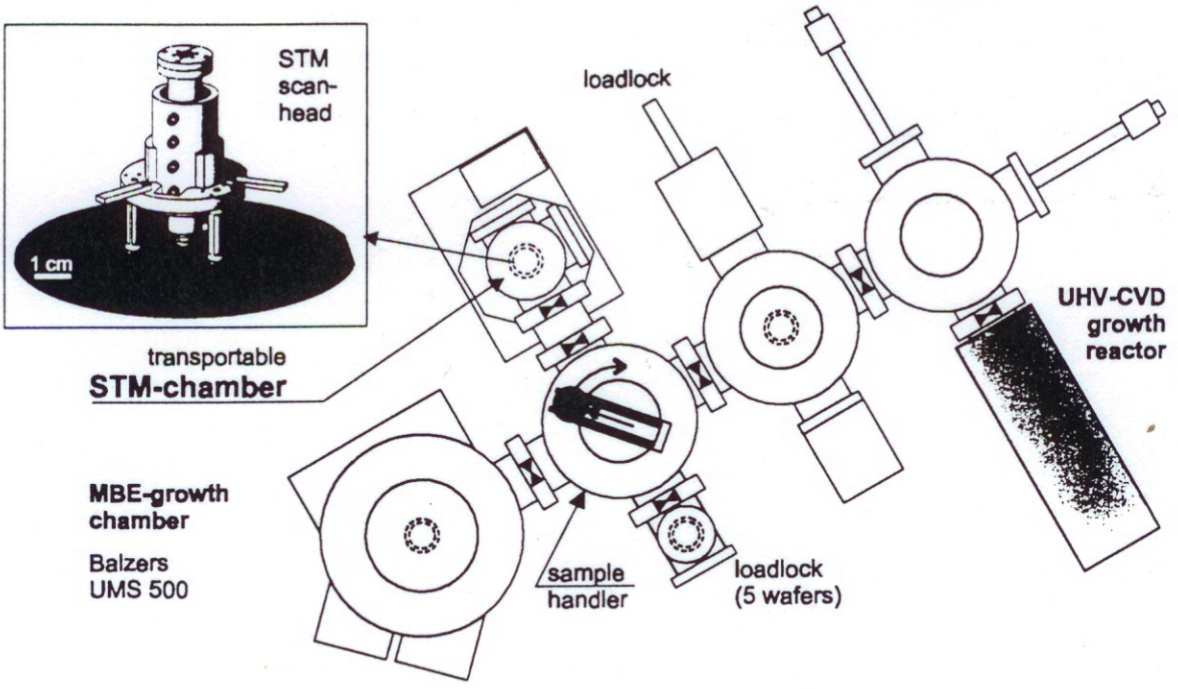

Fig.1: Scheme of the growth system for SiGe-based films, consisting of the MBE-chamber, the sample handler and the UHV-CVD reactor. The transportable STM-chamber is attached to the sample handler for in-situ sample transfer. The inset represents the STM head as described in the text.

transferred in-situ from the growth- to the STM-chamber by means of the sample handler. In order to avoid noise problems due to mechanical vibrations caused by the pumps of the growth system, the STM-chamber is detached from the growth system after the transfer lock has been vented. It is moved to another room for high resolution measurements.

The inset of Fig.1 displays the STM head of the home-built STM. It is based on the Beetle-type microscope originally proposed by Besocke [2] with three outer piezo tubes and a center piezo for scanning. The STM is lowered down directly onto the wafer surface at the desired position. This coarse positioning is done by a standard UHV xyz-manipulator with a range of ±25 mm in the xy-plane. Fine positioning is accomplished by inertial motion of the entire scan head on the wafer and by DC-offset voltages applied to the piezo tubes. Tip approach is effectuated by an Inchworm motor. The tunneling tips are in-situ exchangeable. The STM/sample-holder provides vibration isolation by a spring/eddy-current damping assembly. In addition, the whole chamber resides on laminar flow isolators during measurement. A more detailed description of the STM setup and performance is published elsewhere [3].

Growth procedure

Si-wafers are wet-chemically cleaned followed by an HF-dip for hydrogen passivation before they are loaded into UHV. In the MBE chamber they are heated to 600°C for 10 min for hydrogen desorption followed by a 30 min period at 950°C, resulting in a smooth Si(001) (2x1) surface, which has been confirmed by reflection high energy electron diffraction (RHEED) and STM. At a substrate temperature of 550°C a 200nm thick Si-buffer layer is grown. Onto this buffer carbon is deposited at the same temperature, followed by Ge for the dot layer. Typical deposition rates are $5x10^{-4}$ML/s Carbon at a filament current of about 100A and 0.16 ML/s Ge from the e-gun evaporator. The layer thickness has been varied between 0 ML to 0.17 ML C and 2.5 - 5.8 ML Ge in the samples discussed in this paper. The base pressure of the MBE chamber is

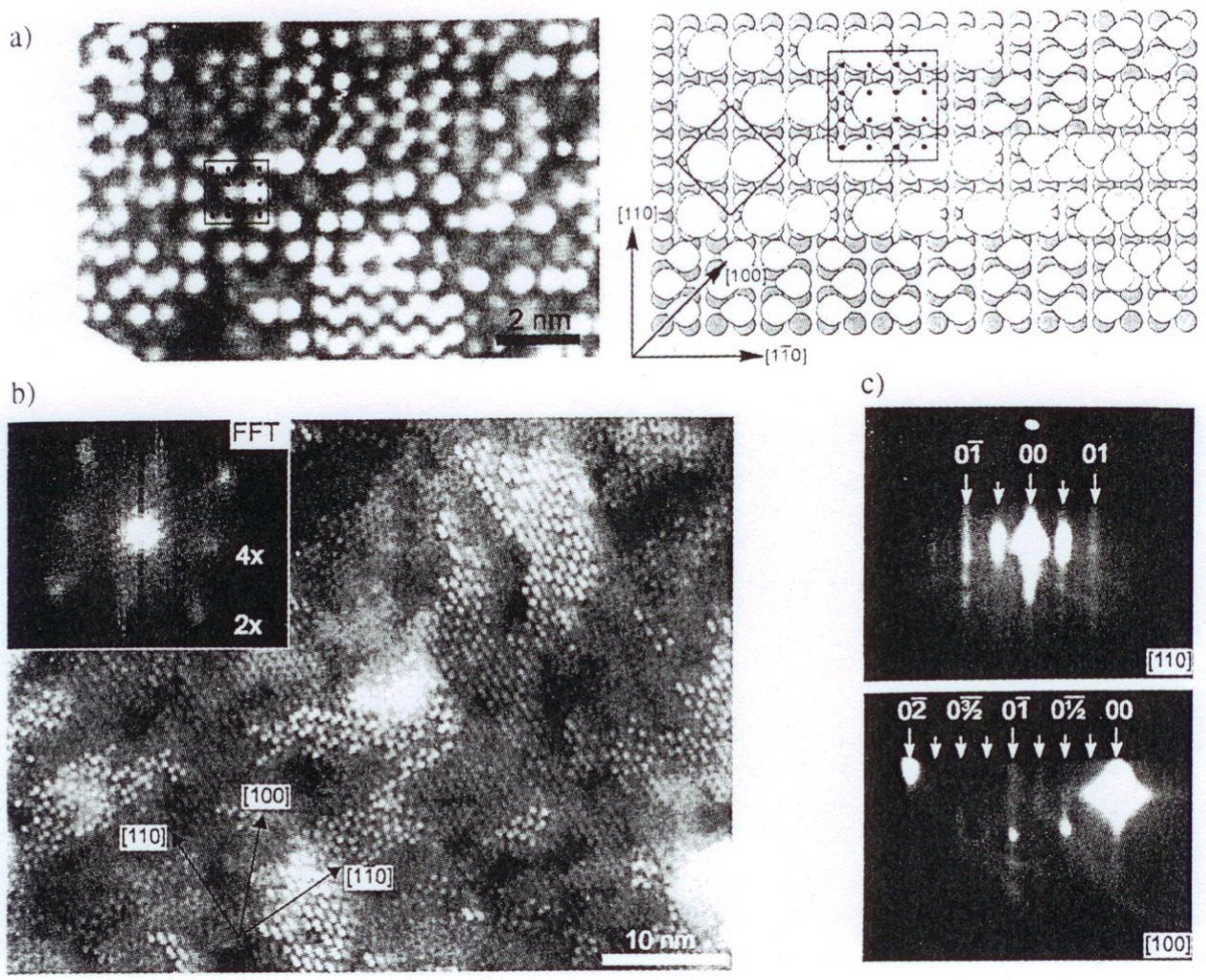

Fig. 2: Carbon induced c(4x4)-reconstruction. **a)** high resolution STM-micrograph showing the c(4x4) structure (bright double-spots) in coexistence with buckled Si-Dimers (smaller zigzag-pattern). A corresponding model is given aside, indicating the c(4x4) unit cell and a primitive one. **b)** larger scan area with c(4x4)-domains on different terraces (inset: Fast Fourier Transform of the image revealing the c(4x4) symmetry in reciprocal space. **c)** RHEED pattern proofing the long range order of the c(4x4) structure. 3 fractional order superstructure streaks can be observed in between the main streaks in [100]-azimuth.

lower than $1x10^{-10}$ mbar and raises to $1x10^{-8}$ mbar during carbon source operation. After deposition, the sample is cooled to RT and transferred to the STM with a chamber pressure of $1x10^{-10}$ mbar.

RESULTS

Carbon covered Si(001)

In a first step, the influence of the C pre-deposition on the clean Si(001) (2x1) surface has been studied in the range of 0.05 to 0.11 ML C. Filled state STM images of a surface covered with 0.11 ML C are displayed in Fig.2 a and b. Aside from an increase in surface roughness, they reveal areas of a surface reconstruction that differs from the well known (2x1) dimer reconstruction of Si(001). It has a unit cell of four by four Si(001) in-plane lattice constants (a_0 = 3.84Å) with a centered symmetry, thus called c(4x4) following the Wood-notation. In the large scale STM image, the c(4x4) patches are those covered with the elongated double-spots running parallel to the <110>-directions. In the RHEED pattern (Fig.2c) three fractional-order spots arising from the c(4x4) superstructure are observed between the main streaks in the [100]-azimuth. In a <110>-

azimuth, i.e. with the electron beam directed parallel or perpendicular to the dimer rows, only one half-order streak is obtained, caused by the centered symmetry. As RHEED is a non-local probe, this confirms the long-range order of the c(4x4) reconstruction. The high-resolution image and the schematic drawing in Fig.2a allow to determine the arrangement of the c(4x4) double-spots with respect to the Si-(2x1) buckled dimer rows (oval zigzag pattern). They are perfectly aligned with the Si-dimers in the same atomic layer. Neighboring rows are shifted to each other by two a_0. The center of the double-bumps and the voids between two of them are always aligned to the middle of the dimer rows in the underlying ML. A c(4x4) unit-cell is represented by the square. The black dots illustrate the non-reconstructed (bulk) positions of single adatoms in that layer. The rhombus indicates a primitive unit cell. A c(4x4)-reconstruction on Si(001), that looks similar to the one observed in this study, has been reported by various authors in the past. It has been prepared by exposure of Si to large amounts of hydrogen at temperatures as high as 700°C [4,5]. In these studies the reconstruction was always referred to as a metastable pure silicon surface, as H is not present at Si surfaces at these temperatures. Only recently it has been suggested that it might be related to C-contamination [6], derived from RHEED experiments. The fact, that the area covered by the c(4x4) pattern scales with the amount of deposited carbon, provides clear evidence that it stems from C-atoms.

Ge deposition onto C-pre-covered Si(001)

In a second step, Ge has been evaporated onto samples with 0.11 ML pre-deposited C at 550°C. This allows to investigate the influence of the C-induced restructuring on Ge island nucleation and to compare it to Ge on a bare Si(001) (2x1) surface. Ge coverages in the range of 2.5 ML to 5.8 ML were used. Fig.3 shows two such layers at Ge coverages of a) 2.5 ML and b) 4 ML. Already at nominally 2.5 ML three-dimensional growth is observed. For simplicity we call these islands Ge/C-dots. Island heights as high as 1.2 nm are observed already at this low coverage. The islands have an irregular shape and consist microscopically of stepped terraces with variable width. This can be seen in Fig.4a for a 3 ML Ge sample. The onset of 3D growth of Ge/C-dots is well below the critical thickness of island formation for Ge on bare Si(001) (2x1) [7], where Ge exhibits a Stranski-Krastanov (SK) growth mode. There it forms a 2-dimensional layer of up to 4 ML prior to island formation driven by elastic strain relaxation [8]. However, as

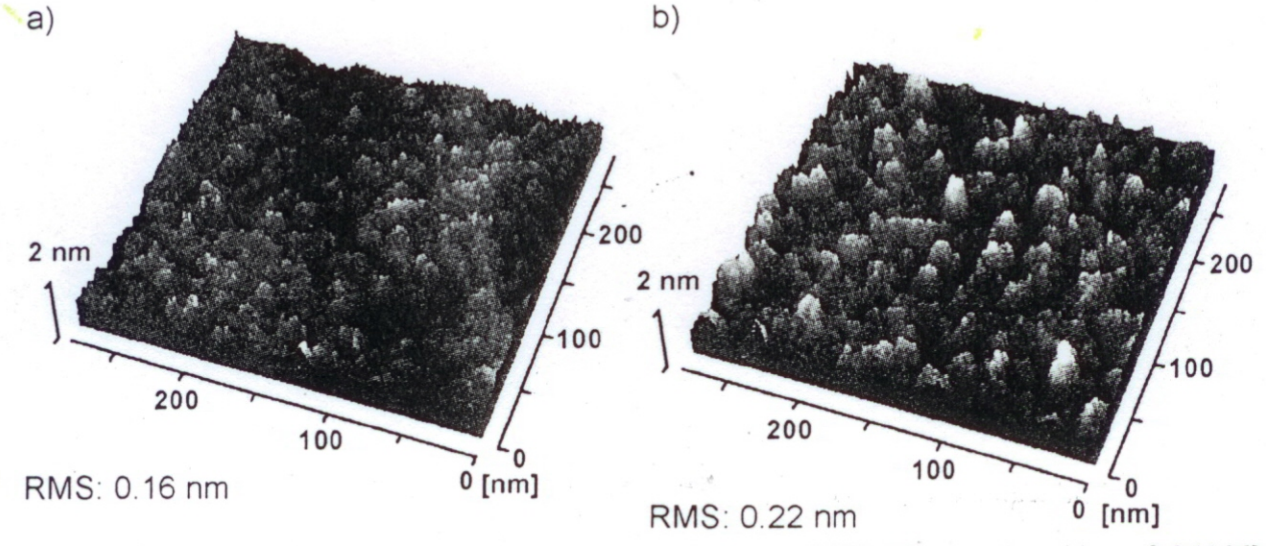

Fig.3: STM-images of Ge-dot-layers deposited onto Si(001) at 550°C after pre-deposition of 0.11 ML C. **a)** 2.5 ML Ge, **b)** 4 ML Ge. Irregularly shaped islands have formed. An increase in island height with Ge-coverage is reflected by the increasing RMS-roughness. The island density remains unchanged at $10^{11}cm^{-2}$.

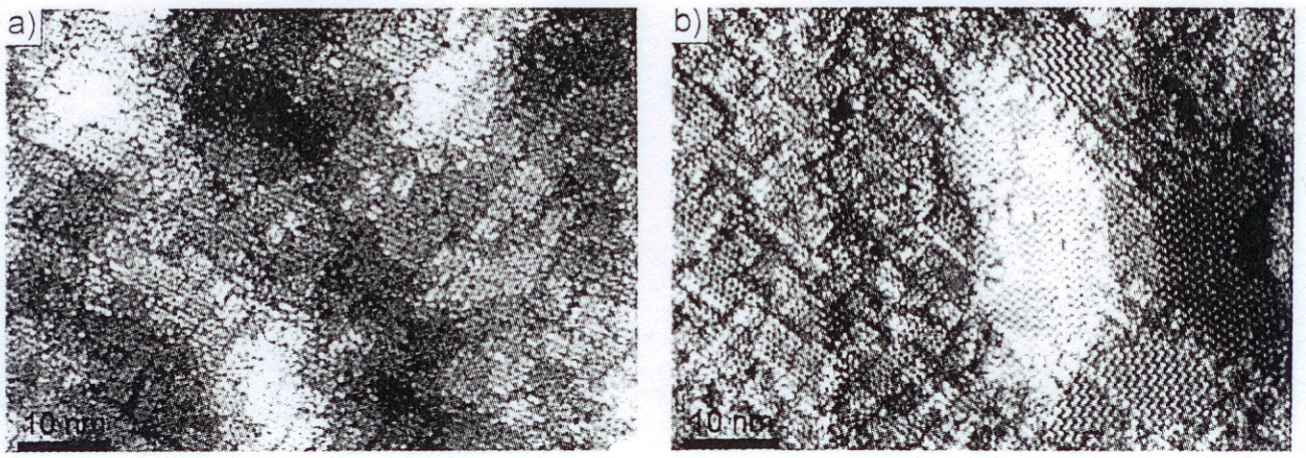

Fig.4: Atomic resolution STM-images of Ge/C-dots. At **a)** 3ML Ge stacks of irregularly stepped terraces with buckled Ge-dimer rows are clearly resolved. Height is 9 ML ~1.2 nm. One distinguishes four islands. At **b)** 5.8 ML Ge larger 'Hut-Cluster'-like islands occur exhibiting {105}-side facets and a (001)-top facet.

C reduces the overall amount of strain in the Ge/C-dot layer, strain is considered not to be the dominating driving force for the earlier onset of island formation. The additional substrate roughness introduced by C as compared to clean Si(001) (2x1) may be an explanation. Moreover, the formation of C-rich surface patches may have an impact on the island formation. On one hand the repulsive forces between Ge and C may lead to an agglomeration of Ge atoms in the areas between the patches. On the other hand, it might be favorable for Ge atoms to stay on the C-rich areas in order to relieve strain.

Increasing the Ge coverage further, the Ge/C-dots grow in height and width, which is obvious in Fig.3b for 4 ML Ge, where the stacks reach a height up to 14 ML ~1.9 nm. The measured root mean square roughness (RMS) rises monotonically from (0.07±0.02)nm for the C-pre-covered Si to (0.22±0.03)nm for the Ge/C-dot layer. The dots still reveal the same irregular shape. The dot density, although somewhat difficult to determine on this rugged surface, remains constant at $10^{11}cm^{-2}$ from 2.5 ML to 4 ML Ge, if only stacks are considered that are higher than the mean height in the STM-images plus the RMS-value. This can be explained by the changed nucleation kinetics on the C-covered surface compared to bare Si(001). We speculate, that the number of nucleation centers is determined by the amount of pre-deposited carbon, and that a variation of the C-coverage can influence the resulting island density.

Up to here, no sign of facet formation is observed, as it might be anticipated from the well known growth behavior of Ge on Si(001) [9]. At a coverage of 5.8 ML Ge, however, the critical thickness for facet formation is reached even for the Ge/C-dots. Dot geometries very similar to the well known 'hut clusters' with quadratic as well as rectangular shape are obtained, as shown in Fig.5a. The size range is 20 nm to 40 nm. At the same time, the surface between the islands smoothens and the terraced islands die out. Fig.4b demonstrates the facet geometry of such a faceted Ge/C-dot. {105}-side facets with their distinctive zigzag reconstruction are well resolved. In addition, all faceted Ge/C-dots observed exhibit a (001)-top facet. This facet shows the characteristic buckled Ge-dimer chains with rows of missing dimers across them. Such missing dimer rows are also observed in the 2D-layers of Ge on Si(001) [10] and are an effective way for relaxation of compressive strain. Thus we conclude, that this type of faceted Ge/C-dots may still contain a significant amount of strain. This is a difference to hut-clusters on bare Si that are completely relaxed towards their apex [11]. Nevertheless we assume, that the mechanism for facet formation is essentially the same as for pure Ge/Si hut-clusters, namely a reduction in sur-

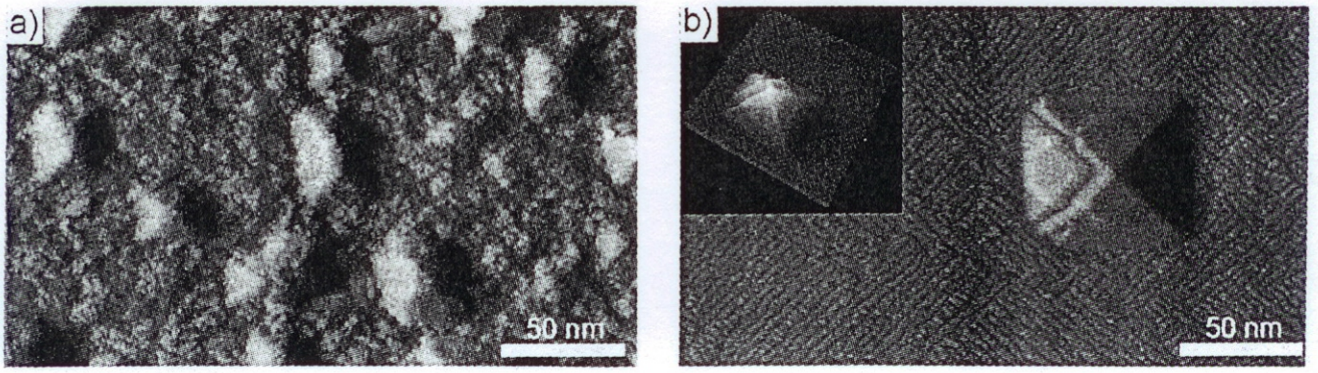

Fig.5: {105}-faceted dots ('hut-clusters') obtained by deposition of 5.8 ML Ge at 550°C **a)** on Si(001) with 0.11 ML pre-deposited C and **b)** on bare Si(001) (2x1). Dot density is at least one order of magnitude larger with C pre-deposition. Ge/C-dot sizes are significantly smaller. The ghostimage on the left slope of the large Ge-dot in b) is a doubletip artifact.

face free energy [12]. As the faceted dots grow at the expense of the terraced Ge/C-dots, their density is a factor of 4 smaller.

For comparison, a sample of 5.8 ML Ge was grown on a clean Si(001) (2x1) substrate at the same growth conditions (Fig. 5b). Here quadratic pyramidal {105}-faceted 'hut-clusters' with essentially uniform sizes about 65 - 70 nm are obtained on a smooth 2D-wetting layer with typical superstructure [10]. Their density is at least one order of magnitude lower than that of their Ge/C-equivalents ($\sim 10^9 cm^{-2}$). It is interesting to note, that this dots seem to grow layer by layer from top to bottom, since the collar-like structure was observed with STM on every dot.

CONCLUSIONS

We have studied submonolayer coverages of C and C-induced Ge dot layers on Si(001) with STM. A C-induced c(4x4)-reconstruction is found at 0.11 ML C on a generally roughened surface. Ge growth on this surface evolves by 3D-island formation already at coverages as low as 2.5 ML in contrast to Ge on bare Si(001) (2x1). Islands consist of irregularly stepped terraces. Their size increases with Ge coverage while their density remains constant. For 5.8 ML Ge the critical thickness for relaxation via {105}-facet formation is exceeded, for both, C-pre-covered and clean Si(001). Island density then reduces by a factor of 4.

REFERENCES

1 O.G. Schmidt, C. Lange, K. Eberl, O. Kienzle, and F. Ernst, Appl. Phys. Lett. 71, 2340 (1997)
2. K. Besocke, Surf. Sci. **181**, 145 (1987)
3. O. Leifeld, B. Müller, D.A. Grützmacher, and K. Kern, Appl. Phys. A **66**(3), S993, (1998)
4. T. Ide, and T. Mizutani,
5. R.I.G. Uhrberg, J.E. Northrup, D.K. Biegelsen, R.D. Bringans, and L.E. Swartz, Phys. Rev.B **46**(16), 10251 (1992)
6. K. Miki, K. Sakamoto, and T. Sakamoto, Appl. Phys. Lett. **71**(22), 3266 (1997)
7. Y.-W. Mo, D.E. Savage, B.S. Swartzentruber, and M.G. Lagally, Phys. Rev. Lett. **65**(8), 1020 (1990)

8. D.J. Eaglesham, and M. Cerullo, Phys. Rev. Lett. **64**(16), 1943 (1990)
9. M. Tomori, K. Watanabe, M. Kobayashi, O. Nishikawa, Appl. Surf. Sci. **76/77**, 322 (1994)
10. U. Köhler, O. Jusko, G. Pietsch, B. Müller, and M. Henzler, Surf. Sci. **248**, 321 (1991)
11. A.J. Steinfort, P.M.L.O. Scholte, A. Ettema, F. Tuinstra, M. Nielsen, E. Landmark, D.M. Smilgies, R. Feidenhans'l, G. Falkenberg, L. Seehofer, and R.L.Johnson, Phys. Rev. Lett. **77**(10), 2009 (1996)